MECHANICAL CHARACTERISTICS OF DEBRIS FLOW

Masaru IWAMOTO and Muneo HIRANO

Forestry and Forest Products Research Institute, Japan

Introduction

Results of experiments and field observations have shown that debris flow tends to form a bore with a swollen front. The bore itself is a non-steady flow, but it can be treated as a steady flow when considered in the co-ordinate system which moves at the same speed as that of bore (see, Fig.1). In actual laboratory conditions,though it is difficult to move the instruments at the same speed as the bore, and even if this can be achieved, the bore reaches the downstream end within a short space of time, and so allows observation only for a very limited period of time during which is moving at high speed. However moving the bed against the flow ensures keeping the bore stationary and makes it possible to observe it with increased accuracy for a long period of time. With this in mind, a belt-conveyor type of channel was constructed to test the behaviour of the bore.

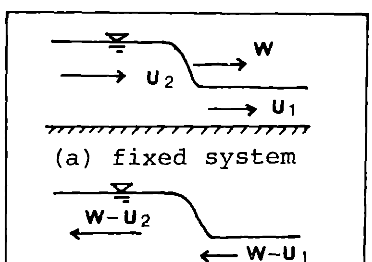

Fig. 1 Co-ordinate system

Masaru IWAMOTO
Researcher, Dr. Agr., P.O.Box 16,
Tsukuba, Ibaraki, 305, Japan

Muneo HIRANO
Associate Professor of Civil Engineering, Dr. Eng., Kyushu University,
Fukuoka,812, Japan

Experimental Methods

The belt-conveyor type of channel measuring 2 m long, 10 cm wide and 20 cm high was constructed with sides of acrylite walls and a belt in close contact with the bed. The layout of the equipment is shown in Fig. 2. The belt had an adjustable speed ranging from 0 to 2 $m \cdot s^{-1}$, while its slope, tan θ, could be varied from 0 to 0.5. In order to generate a bore, water and grains were fed into the upstream end of the moving belt. The bore was then made to stand still through adjustment of the belt speed, bed slope and the amount of water supplied.

An optimum combination of belt speed, bed slope and water supply rate enabled the average position of the bore end to be kept constant and it was able to be regarded as a stationary bore. Consequently as the shape of the bore does not change on the average, the discharge and mean velocity become zero all over the channel. Though a circular type of channel which incorporates a moving bed is often adopted, this channel does not have a slope range as extensive as that of the belt-conveyor type of channel. The belt-conveyor type of channel has the following advantages over those channels formally used

(1) A flow of selected velocity can be set up with a selected slope. For instance, a flow of zero mean velocity, a flow with zero velocity on its surface and a uniform flow against reversed slope are all obtainable with ease.

(2) When grains are present, detailed and prolonged observation of grain behaviour is possible with increased accuracy of measurement, by setting up the flow with equivalent velocity to that of the grain. For instance, in the flow where V_m = 100 $cm \cdot s^{-1}$, if grains A and B have the slightly different velocities of V_A = 102 $cm \cdot s^{-1}$ and V_B = 98 $cm \cdot s^{-1}$ respectively, it is easy to come to the conclusion

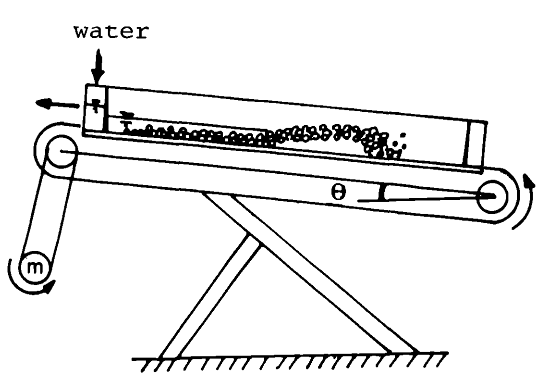

Fig.2 Experimental apparatus

that $V_A > V_m > V_B$ because in the flow with velocity, $V_m = 0$ grain A moves downstream at $V_A = 2\ cm \cdot s^{-1}$ while grain B moves upstream at $V_B = 2\ cm \cdot s^{-1}$

Results and Discussion

Shape of debris flow

The shapes of those hydraulic bores composed of only water and a mixture of water and mesalight grains (8.2 mm in diameter, specific gravity of 1.55) were photographed by a motor-driven camera and analyzed. The shapes of the bores are shown in Figs. 3 and 4 respectively. From the figures, it is seen that in general, because of the increase of shearing force near the bed, the bore tends to form a steep standing front which is in proportion to the increase of water depth, channel slope and belt speed. The bore which also contains the mesalight grains has a standing front larger and steeper than the water bore because air is able to filter through it more readily.

As the bore looks stationary in this channel, a model of steady bore can be illustrated as seen in Fig. 5. In the figure, equations of motion and continuity are as follows

$$u\frac{\partial u}{\partial x} + v\frac{\partial u}{\partial y} = g \sin\theta - \frac{1}{\rho}\frac{\partial p}{\partial x} + \frac{1}{\rho}\frac{\partial \tau}{\partial y} \qquad (1)$$

$$u\frac{\partial v}{\partial x} + v\frac{\partial v}{\partial y} = -g \cos\theta - \frac{1}{\rho}\frac{\partial p}{\partial y} \qquad (2)$$

and

$$\frac{\partial u}{\partial x} + \frac{\partial v}{\partial y} = 0 \qquad (3)$$

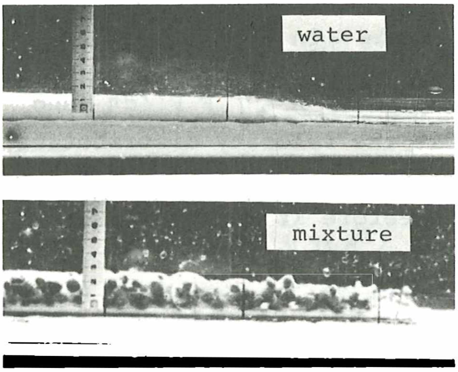

Fig.3 Shapes of bore

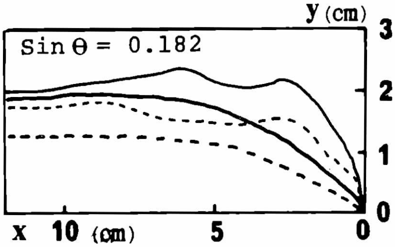

V_B	227.9	141.6
water	———	------
mixture	———	

Fig.4 Shapes of bore

where, u and v are the component of velocity in the direction of x and y axes respectively, p is the pressure, τ is the shear stress, ρ is the flow density and h is the depth of flow. Considering the stream function as follows,

$$\Psi = u_o\, h\, F(\eta), \qquad \eta = y/h \tag{4}$$

then u and v are defined respectively

$$u = u_o F' \qquad v = u_o \frac{dh}{dx}(\eta F' - F) \tag{5}$$

where u_o is the surface velocity assumed equal at any point on the bore.
Applying Eqs. 4 and 5 to Eq. 1, the following relation is obtained

$$\frac{p}{\rho g h} = (1-\frac{y}{h})\cos\theta + \frac{u_o^2}{g}\cdot\frac{d^2h}{dx^2}\int_\eta^1 F'(\eta F'-F)\,d\eta - \frac{u_o^2}{gh}\left(\frac{dh}{dx}\right)^2\int_\eta^1 \eta F F''\,d\eta \tag{6}$$

Adopting Prandtl's mixing length theory, one gets shear stress

$$\tau = \rho\, l^2\left(\frac{du}{dy}\right)^2 = \rho\, l^2\,\frac{F''}{h^2}\,u_o^{\ 2} \tag{7}$$

where l is the mixing length. If one considers $l = K\,h$ (K: constant), then Eq. 8 is obtained.

$$\tau = \rho\, K^2\, F''\, u_o^2 \tag{8}$$

Eq. 8 shows that the shear stress on the bed, τ_o is constant regardless of x.
Given that $\tau_o = \rho g h_o \sin\theta$ and the pressure is the hydrostatic distribution, i.e., the left side in Eq. 2 is zero, if one calculates Eq. 6 where x = 0 and h = 0, then the following analytical equation is obtained.

$$\frac{x}{h_o}\tan\theta = \frac{h}{h_o} + \left(1-\frac{F_o^2\cdot A}{\cos\theta}\right)\ln\left(1-\frac{h}{h_o}\right) \tag{9}$$

where h_o is the depth from a base plane, $A = \int_0^1 F\,F''\,d\eta$ and $F_o^2 = u_o^2/gh_o$ If one assumes that the velocity distribution is a parabolic curve, then one finds that values calculated from Eq. 6 and 9 are equal. Therefore it may be thought that the pressure in bore is the hydrostatic distribution.
In Fig. 6, the curve computed from Eq. 9 by assuming that A = -0.03 is compared with the observed curve. Seeing that the agreement is fairly good, it may be concluded that the assumptions made in Eqs. 4 - 9 are reasonable.

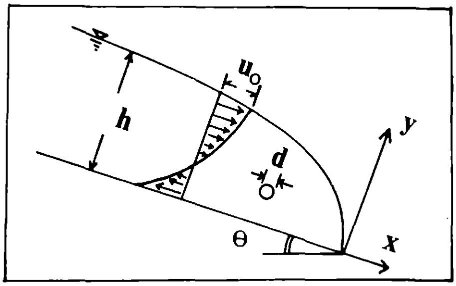

Fig.5 Definition sketch

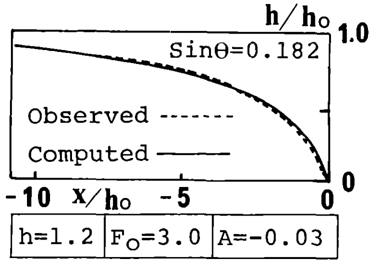

Fig.6 Comparison of computed values h/h_o with the experimental results

Concentration of debris flow

Samples were collected by inserting a cylinder into the debris flow as shown in Fig. 7. The belt was brought to a halt as soon as the cylinder was in position. Following this, the concentration was obtained by measuring the height of debris flow, h and grain depth in the cylinder, h_* with the following expression;

$$C_m / C_* = h_* / h \tag{10}$$

where C_m is the mean concentration and C_* is the maximum possible concentration of the debris.

Fig. 8 shows the observed values and it can be seen that, in this experiment, the mean concentration was found to be almost unvarying, regardless of the angle of the bed slope and the belt speed.

The distribution of grain concentration was calculated from a photograph by counting the number of grains in contact with the side wall.

A small area with a length of l and a height of Δh_l was then marked off on the side wall as shown in Fig.9. Assuming that the number of grains in contact with the area is n and the the number of grains in a cube of $l \times l \times \Delta h_l$ is N, then N is considered to be proportional to n^2 and thus the concentration in the cube, C is given by the following equation

$$C = \frac{N \pi d^3 / 6}{l^2 \cdot \Delta h_l} \propto \frac{n^2 \; d^3}{l^2 \cdot \Delta h_l} \tag{11}$$

where d is the diameter of grain. When the grains are uniform in size

$$C / C_o = (n / n_o)^2 \tag{12}$$

where C_o and n_o are the concentration and the number of grains at the standard level respectively.
Fig.10 shows the distribution of the concentration obtained from Eq.12 wherein l equals 10 cm and Δh_1 equals 1 cm.

The concentration of the grains is found to be fairly even except near the bed where it is found to be lower than that of the upper part, unlike the suspended load.

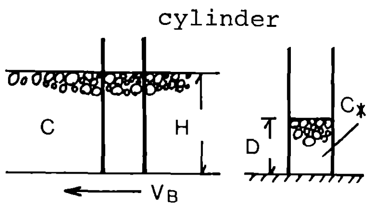

Fig.7 Measurement of concentration

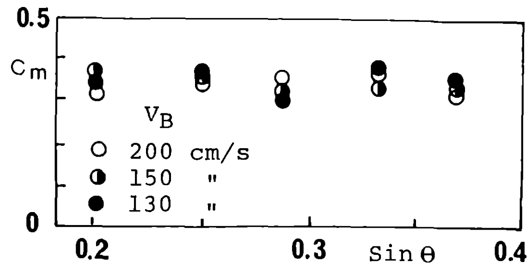

Fig.8 Mean concentration of debris flow

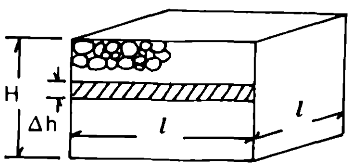

Fig.9 Definition sketch

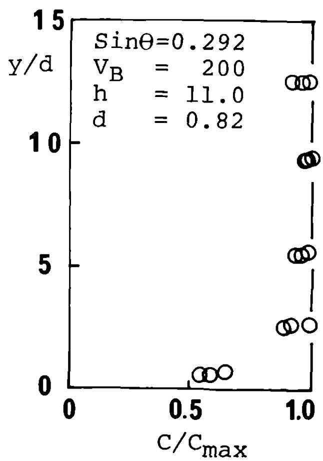

Fig.10 Distribution of concentration

Velocity distribution of debris flow

The velocity of the grains in the moving co-ordinate system was measured by a camera and is shown in Fig.11. In the figure, the upper grains were seen to be moving downstream, while the lower ones, upstream. However, the velocity distribution in a fixed co-ordinate system could also be obtained, by adding the belt speed to the grain velocity as shown in Fig.12. In the figure, although the velocity distribution appears uniform and looks like the Bingham flow, in this system, it is as is apparent from Fig.11, not the Bingham flow but a shear flow. The above shows that one of the advantages of the belt-conveyor type of channel is that it permits the detection of very slight velocity difference which can hardly be measured in the usual type of channel.

Further, Fig.11 shows that the grains tend to slip on the bed surface. Bagnold(1954) carried out grain dispersion experiments in an annulus with a rotating outer boundary, but as he failed to take account of the grain slippage at the boundaries in calculations, the validity of his results should be reconsidered.

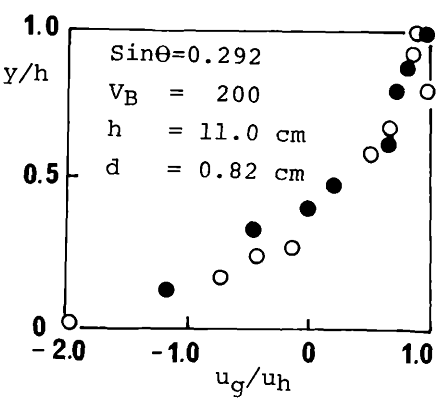

Fig.11 Velocity distributon of debris flow in a moving co-ordinate system

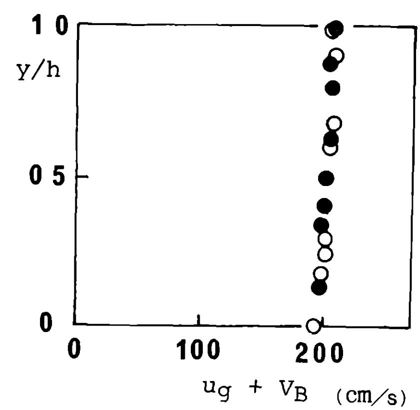

Fig.12 Velocity distribution in a fixed co-ordinate system

(u_g average velocity of grain, V_B belt speed, d grain diameter, u_h velocity at the surface, h flow depth and y distance from the bed)

Sorting of grains at the debris front

(1) In the field, the concentrated large grains have frequently been observed at the front of rocky debris flow. Fig.13 shows one of the typical shapes of debris flow composed of mixed mesa-light grains from 3.5 mm to 12.7 mm in diameter. In the figure, one can easily observe the concentrated large grains

both on the surface and at the front of debris flow and their grain distributions at the same time are shown in Fig.14. The figure shows the differences of the grain distribution among them and also the reverse grading which is common in shear flow sedimentation.

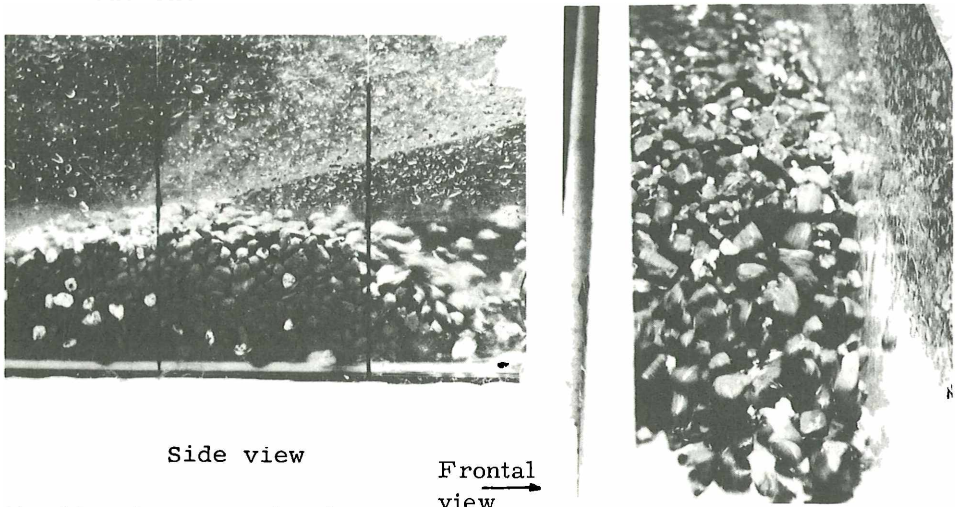

Fig.13 Shape at the front

The trajectories of the grains measured by VTR are shown in Fig.15. It can be seen that, due to velocity distribution,a grain which has fallen to the lower part travels upstream and moves again downstream in the upper area, and in this way, grains are seen to be re-circulating continuously in the debris flow.

Once the upper grains arrive at the front, they drop to the bed and get caught up into the flow near the bed, to be carried back upstream. However, as large grains are more resistant to being caught into the flow than small ones, they tend to remain at the front throughout.

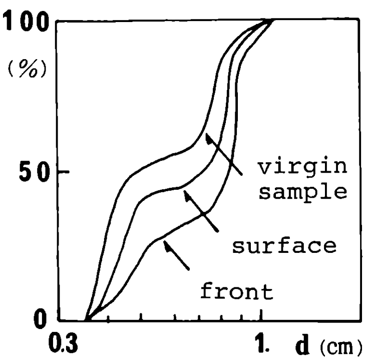

Fig.14 Grain size distribution

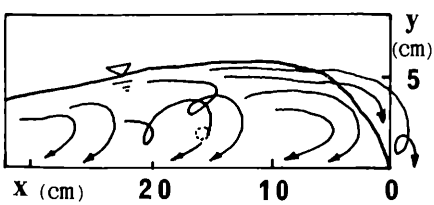

Fig.15 Trajectories of grains

This, therefore, accounts for the occurrence of a concentration of large grains at the front of the debris flow.

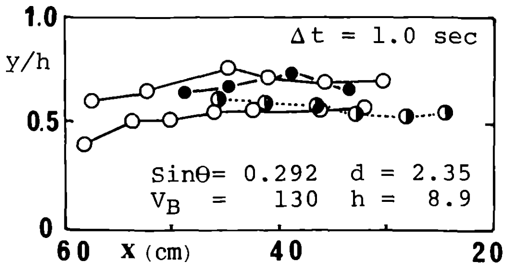

Fig.16 Trajectories of large grains

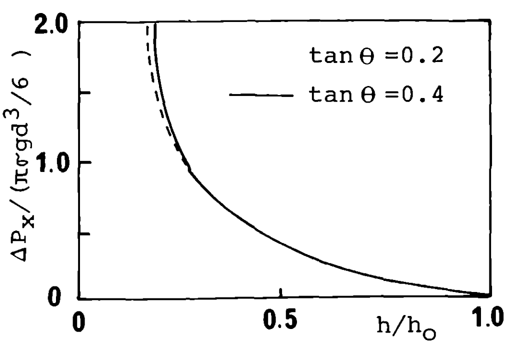

Fig.17 Pressure acting on the grain

(2) Further, in order to take a clear trajectory of large grains, several large grains of 23.5 mm in diameter were put into a flow of homogeneous grains 8.2 mm in diameter. Fig.16 shows the trajectories of these large grains. From the figure, it can be seen that grains followed a path parallel both to each other and the bed, rather than moving in a depthwise direction.

Given this information then, the following assumption about the difference in pressure, ΔP_x, may be considered;

$$\Delta P_x = - K_1 \, d^3 \frac{\partial P}{\partial x} \qquad (13)$$

where K_1 is the constant. This equation means that when a grain, d in diameter, moves in the flow, the pressure difference in front of and behind the grain and the acting area is proportional to $-(\partial p/\partial x)\, d$ and d^2 respectively. ΔP_x acts on the grain as the accelerating force because $\partial p/\partial x$ is negative at the debris front and ΔP_x acts downwards. Given that its pressure distribution is hydrostatic in Eq.6, then one can estimate the magnitude of ΔP_x by computing the ratio of ΔP_x to gravity, as shown in Fig.17. The figure shows that the ratio shows a gradual increase towards the front and the pressure effect becomes considerable.

Hence it may be considered that this pressure difference is also one of the reasons for the occurrence of large grain concentration at the front.

Conclusions

(1) Although debris flow is a non-steady flow in itself, it can be treated as a steady flow in a moving co-ordinate system, i.e., the belt-conveyor type of channel, and thus achieve increased accuracy of measuring.

(2) The shape of the debris flow is computed by the equations of motion and continuity assuming that the stream function, the shear stress and the pressure distribution are Eqs.4 7 respectively and are all hydrostatic. This shows good agreement with the flume data.

(3) In this experiment, the mean concentration of debris at the front was found to be almost always unvarying, regardless of an angle of bed slope and belt speed. The distribution of concentration is uniform except close to the bed, where unlike the case of the suspended load, the concentration is lower than that of the upper part.

(4) Though the velocity distribution of debris flow seems uniform and looks like the Bingham flow in the fixed co-ordinate system, it is as is apparent from Fig.11 not the Bingham flow but a shear flow.

(5) As large grains have a greater amount of pressure behind them than small ones, they tend to be propelled fast to the front of the flow, where they stay as they are more resistant to being caught up in the flow than small ones. These functions explain the occurrence of large grain concentration at the front of the flow.

S u m m a r y

In the past ten years, numerous studies on the occurring criteria, flowing characteristics and depositing processes of debris flow have been carried out both in the laboratory and in field observations at Mt. Sakurashima and Mt. Yake (Japan). Although various significant results have been obtained, some details of the kinetic mechanisms still need further investigation. The characteristics of the front of the debris flow is one of these significant problems.

Debris flow generally tends to form a non-steady bore with a swollen front. Because the rapid motion of the bore is difficult to measure accurately in the usual type of channel, a belt-conveyor type of channel was constructed. This made it possible to observe the debris flow over a long period of time.

The channel, incorporating a belt moving against the flow of the bore, was able to turn a non-steady flow into a continuous flow which is stationary to the laboratory.

By setting the belt speed equal and opposite to the mean flow velocity for a selected slope, detailed and protracted observation of grain behaviour was possible with increased accuracy of measurement.

Results of these experiments on debris flow, using the belt-conveyor channel, produced various data about the shape, velocity distribution and concentration of debris flow, the sorting of grains at the debris front and the grain trajectories.

Literature Cited

Bagnold, R. A., 1954 Experiments on a gravity-free Dispersion of Large Solid Spheres in a Newtonian Fluid near Shear. Proc. Roy. Soc. London. A. Vol. 225, pp. 49-63.

Hirano, M., Iwamoto, M. & Saruwatari, H., 1978 Some Experimental Studies of Flow in Flume with Belt-conveyor Bed. Proc. 22th Japanese Conf. Hydraulics. pp. 283-289.